JACS
JOURNAL OF THE AMERICAN CHEMICAL SOCIETY
pubs.acs.org/JACS
Communication

Molecular Complexes Featuring Unsupported Dispersion-Enhanced Aluminum−Copper and Gallium−Copper Bonds

Kristian L. Mears, Cary R. Stennett, Elina K. Taskinen, Caroline E. Knapp,* Claire J. Carmalt,* Heikki M. Tuononen,* and Philip P. Power*

Cite This: https://dx.doi.org/10.1021/jacs.0c10099
Read Online

ABSTRACT: The reaction of the copper(I) β-diketiminate copper complex $\{(Cu(BDI^{Mes}))_2(\mu\text{-}C_6H_6)\}$ (BDI^{Mes} = *N*,*N*′-bis(2,4,6-trimethylphenyl)pentane-2,4-diiminate) with the low-valent group 13 metal β-diketiminates $M(BDI^{Dip})$ (M = Al or Ga; BDI^{Dip} = *N*,*N*′-bis(2,6-diisopropylphenyl)pentane-2,4-diiminate) in toluene afforded the complexes $\{(BDI^{Mes})CuAl(BDI^{Dip})\}$ and $\{(BDI^{Mes})$-$CuGa(BDI^{Dip})\}$. These feature unsupported copper−aluminum or copper−gallium bonds with short metal−metal distances, Cu−Al = 2.3010(6) Å and Cu−Ga = 2.2916(5) Å. Density functional theory (DFT) calculations showed that approximately half of the calculated association enthalpies can be attributed to London dispersion forces.

An understanding of the nature of metal−metal bonding in both main group and transition metal systems is of fundamental importance.[1,2] Recently, the discovery of compounds featuring new metal−metal bonding types has been driven not only by curiosity but also by their many potential applications.[3−6] These include their use in C−F bond functionalization,[7] CO_2 activation,[8] electrochemistry,[9] and precursors to thin films for photovoltaic applications.[10] Many notable homometallic-dinuclear compounds have been isolated,[11,12] but scarcer heterobimetallic species have also generated interest as a result of their potential for improved selectivity and reactivity as catalysts.[13] However, most of the examples presented to date use bridging ligands to support the metal−metal bonds, or such bonds are formed as part of a cluster species.[14−17] Some examples include heteroatom (e.g., μ-hydrido) bridges between the metal centers, as seen in the complexes $\{Cu(BDI^{Ar})(H)Au(IPr)\}$ (BDI^{Ar} = *N*,*N*′-bis(pentafluorophenyl)pentane-2,4-diiminate; IPr = 1,3-diisopropylphenylimidazol-2-ylidene) and $\{Zr(H)$-$(Cp)_2(H)_2M(BDI^{Dip})\}$ (M = Zn, Mg, Al; Cp = cyclopentadienyl; BDI^{Dip} = *N*,*N*′-bis(2,6-diisopropylphenyl)-pentane-2,4-diiminate).[18,19] Recent examples of heterobimetallic complexes with metal−metal bonds include the two-coordinate Mn(0) species $\{Mn(L)(Mg(BDI^{Mes}))\}$ (L = $N(C_6H_2\{C(H)Ph_2\}_2{}^{i}Pr\text{-}2,6,4)(Si^{i}Pr_3)$; BDI^{Mes} = *N*,*N*′-bis(2,4,6-trimethylphenyl)pentane-2,4-diiminate),[20] as well as the palladium complex, $\{Pd(H)_3(Mg(BDI^{Dip})_3\}$.[21] Other examples include unsupported Fe−Mn or Fe−Cr bond formation stabilized by bulky terphenyl ligands,[22] as well as Dy−Fe and Dy−Ru bonds featuring Cp-based ligands for single molecule magnet applications.[23]

A theme that has attracted increased attention is the use of low-valent p-block compounds as "ligands" in heterometallic species to form metal−metal bonds.[24−26] Group 13 based metal(I) ligands in particular have generated interest as synthons for metal−metal bonded compounds.[27−29] Interestingly, in a recent example, a potassium aluminyl complex was reacted with a phosphine-ligated gold iodide species which resulted in the heterobimetallic aluminum−gold complex $\{(NON)AlAu(P^{t}Bu_3)\}$ (NON = 4,5-bis(2,6-diisopropylanilido)-2,7-di-*tert*-butyl-9,9-dimethylxanthene) (**III**, Figure 1).[8]

The strong electron-donating properties of the [(NON)Al] species afforded a highly polarized $Al^{\delta+}$−$Au^{\delta-}$ bond, into which

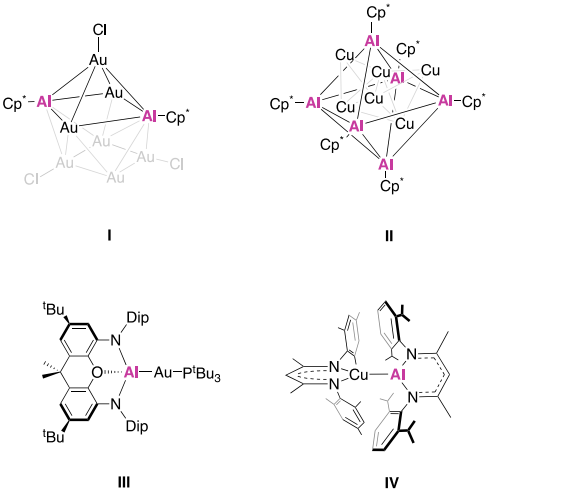

Figure 1. Fragments of previously reported Au−Al and Cu−Al clusters (**I** and **II**, Cp* = C_5Me_5), the first reported monomeric Au−Al unit (**III**, Dip = 2,6-$^{i}Pr_2$-C_6H_3) and a monomeric Cu−Al unit described in this study (**IV**).

Received: September 23, 2020

CO_2 was shown to insert. This work provided the first example of a coinage metal bonded to a low-valent aluminum species to form a discrete bimetallic unit, though some examples of metallic clusters featuring Al−Au bonds (e.g., $[Ni(AuPPh_3)_{(8-2n)}(AuCl)_3(AlCp^*)_n]$, n = 1, 2; Cp* = pentamethylcyclopentadienyl) have been reported (**I**, Figure 1).[30]

There are two examples of compounds that feature bonds between aluminum and copper. These are the clusters reported by Fischer et al. in 2014.[31] $[(Cp^*Al)_4]$ was reacted with $[(Cu(H)(PPh_3))_6]$ to form the intermetallic cluster $[(Cp^*AlCu)_6H_4]$. Subsequent addition of benzonitrile resulted in $[(Cp^*AlCu)_6(H)_3(N{=}CHPh)]$ via a hydrometalation pathway, featuring an $[Al_6Cu_6]$ core (**II**, Figure 1).[31]

Analogous examples of gallium(I) species[32,33] bound to transition metals are known, but to date the only reported instances featuring group 11 metal−gallium bonded moieties were prepared by salt-metatheses of a gallyl anion and a transition metal chloride, stabilized by N-heterocyclic carbene (NHC) or bisphosphine ligands.[34−37] These suggest that by employing low-valent nucleophilic group 13 compounds at group 11 centers, new complexes may be obtained.

Here, we report the synthesis and characterization of the first example of a low-valent Cu−Al molecular complex $\{(BDI^{Mes})CuAl(BDI^{Dip})\}$, **4** via the reaction of a monomeric carbene-analogue of Al with a copper(I) source stabilized by a BDI ligand. Additionally, we report the characterization of its heavier Cu−Ga analogue $\{(BDI^{Mes})CuGa(BDI^{Dip})\}$, **5**.[36,37]

Both $\{(BDI^{Mes})CuAl(BDI^{Dip})\}$, **4**, and $\{(BDI^{Mes})CuGa(BDI^{Dip})\}$, **5**, were synthesized by the reaction of dinuclear $\{(Cu(BDI^{Mes})_2(\mu\text{-}C_6H_6)\}$, **1**,[38] and either $\{Al(BDI^{Dip})\}$, **2**,[39] or $\{Ga(BDI^{Dip})\}$, **3**,[40] at room temperature in toluene (Scheme 1). The resulting orange colored mixtures were

Scheme 1. Synthetic Route to Complex 4 and 5

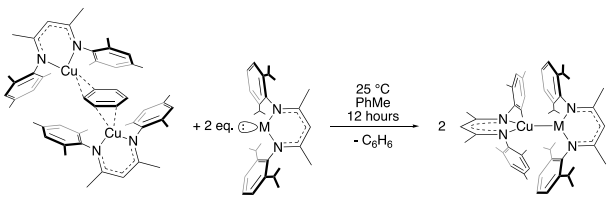

stirred for 12 h. Removal of the solvent under reduced pressure gave **4** or **5** as yellow solids which were extracted in a mixture of toluene/hexane and filtered. The filtrate was concentrated and cooled to ca. −30 °C overnight, yielding complexes **4** or **5** as yellow crystals that were suitable for single-crystal X-ray analysis (Figures 2 and 3). Both **4** and **5** have marginal stability in solution; decomposition occurred at temperatures greater than ca. 80 °C to uncharacterizable black solids. Selected bond lengths and angles for **4** and **5** are shown in Table 1.

BDI^{Mes} was chosen as the ligand at the copper atom as a crystallographic handle to prevent the metal centers being indistinguishable by X-ray analysis, which would probably ensue if BDI^{Dip} was used at both metals. Complex **4** has a significantly shorter Cu−Al distance, 2.3010(6) Å, than the shortest known Cu−Al bond length of 2.4134(15) Å in Fischer's $[Al_6Cu_6]$ cluster (Figure 1), showing a shortening of 4.7%.[31]

The relatively short Cu(1)−Al(1) bond length in **4** is a consequence of the 3s character of the lone pair at the Al

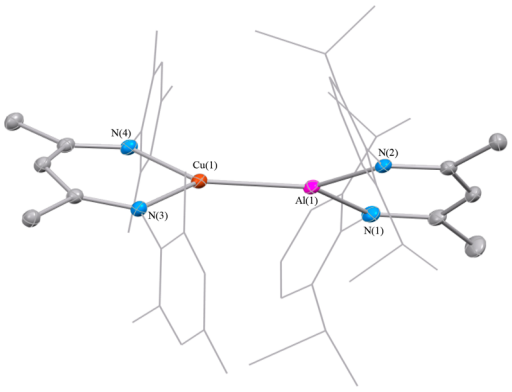

Figure 2. Solid-state structure of $\{(BDI^{Mes})CuAl(BDI^{Dip})\}$, **4**, with hydrogen atoms not shown and Mes/Dip substituents shown in wireframe format for clarity.

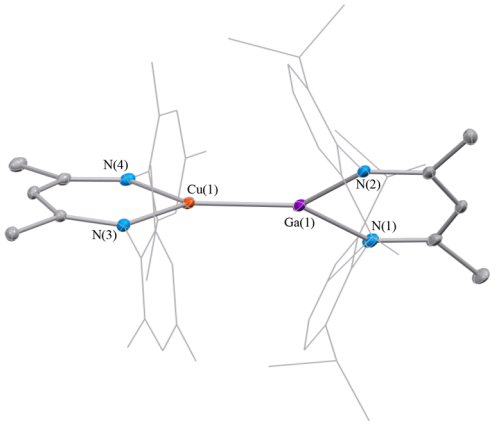

Figure 3. Solid-state structure of $\{(BDI^{Mes})CuGa(BDI^{Dip})\}$, **5**, with hydrogen atoms not shown and Mes/Dip substituents shown in wireframe format for clarity.

Table 1. Selected Bond Lengths and Angles for Complexes 4 and 5[a]

	4 M = Al	**5** M = Ga
Bond Lengths (Å)		
Cu(1)−M(1)	2.3010(6) [2.346]	2.2916(5) [2.340]
M(1)−N(1)	1.9228(17) [1.931]	1.992(3) [2.003]
M(1)−N(2)	1.9213(17) [1.931]	1.985(3) [2.003]
Cu(1)−N(3)	1.9967(15) [2.011]	1.974(2) [1.992]
Cu(1)−N(4)	1.9863(15) [2.011]	1.967(2) [1.992]
Bond Angles (deg)		
Cu(1)−M(1)−N(1)	136.04(6) [134.2]	137.36(9) [134.9]
Cu(1)−M(1)−N(2)	131.45(5) [134.2]	131.56(7) [134.9]
M(1)−Cu(1)−N(3)	131.84(5) [132.1]	131.22(7) [131.2]
M(1)−Cu(1)−N(4)	131.95(5) [132.1]	130.49(7) [131.2]
N(2)−M(1)−N(1)	92.51(7) [91.7]	91.06(11) [90.2]
N(4)−Cu(1)−N(3)	96.21(6) [95.8]	98.28(9) [97.5]

[a]Calculated values in square brackets.

atom.[30] The Al(+1) electron configuration can be described as $3s^2$, in which the 3s-orbital has a smaller radius than the 3p-orbital. This effect was also observed by Aldridge and coworkers in $\{(NON)AlAu(P^tBu_3)\}$,[8] which has a shorter Al−Au bond length of 2.4024(3) Å in comparison to the Al−Au length of 2.596(5) Å in the Al−Au cluster (Figure 1),[29] a shortening of 7.5%.

https://dx.doi.org/10.1021/jacs.0c10099
J. Am. Chem. Soc. XXXX, XXX, XXX−XXX

The Al(1)−N(1) and Al(1)−N(2) bond lengths (1.9228(17) and 1.9213(17) Å, respectively) in **4** are shorter than those (1.957(2) and 1.957(2) Å) in **2**. In contrast, the Cu(1)−N(3) and Cu(1)−N(4) bond lengths (1.9967(15) and 1.9863(15) Å) in **4** are much longer than those in **1** (1.931(2) and 1.912(1) Å). The N(2)−Al(1)−N(1) bond angle in **4** (92.51(7)°), is slightly wider than in **2** (89.96(8))°. The opposite is true for the copper fragment where there is a narrower N(4)−Cu(1)−N(3) bond angle (96.21(6)°) in contrast to **1** (98.9(1) and 99.39(9)°). This trend holds for **5**, which has a wider N(2)−Ga(1)−N(1) bond angle (91.06(11)°) compared to **3** (87.53(5)°) and a slightly narrower N(4)−Cu(1)−N(3) angle (98.28(9)°).

The changes in the bond lengths and angles that occur at Al and Cu upon the formation of complex **4** are presumably a consequence of transfer of electron density from Al to Cu, which increases the ionic character of the Al−N bonds causing them to shorten and the N−Al−N angle to widen. The opposite happens at Cu where electron density is increased and ionic character of the Cu−N bonds is lowered.

The gallium analogue **5** has a Cu−Ga bond length of 2.2916(5) Å, which is similar to the Cu−Al distance but slightly shorter than that reported by Jones and co-workers for the related complex {(IMes)Cu{Ga{[N(Dip)C(H)$_2$]}}} (IMes = 1,3-dimesitylimidazol-2-ylidene), 2.3066(6) Å.[34] The charge difference between the Ga fragments in **5** and Jones' {(IMes)Cu{Ga{[N(Dip)C(H)$_2$]}}}, 0 and −1, respectively, may account for the shorter Cu−Ga bond length in **5**. However, they also showed that lowering the steric bulk on the NHC substituent in {(IPr)Cu{Ga{[N(Dip)C(H)$_2$]}}} gave an even shorter Cu−Ga bond length of 2.2807(5) Å. The Ga(1)−N(1) and Ga(1)−N(2) bond lengths in **5** (1.992(3) and 1.985(3) Å) are shorter than those (2.0528(14) and 2.0560(13) Å) in **3**. In comparison with the starting material **1**, **5** shows significant lengthening of Cu(1)−N(3) and Cu(1)−N(4) bonds (1.974(2) and 1.967(2) Å, respectively).

Computational studies using dispersion-corrected density functional theory (DFT) at the PBE1PBE-D3BJ/def2-TZVP level gave interaction enthalpies (free energies) of 221 (131) and 192 (106) kJ mol^{-1} for **4** and **5**, respectively. Approximately 50% of the calculated interaction enthalpies can be assigned to London Dispersion Forces (LDFs) between the BDI^{Mes} and BDI^{Dip} ligands (109 and 106 kJ mol^{-1} for M = Al and Ga, respectively). More detailed bonding analyses using the extended transition state method with natural orbitals for chemical valence (ETS-NOCV) further showed that the electrostatic (−463 and −372 kJ mol^{-1}) and orbital (−169 and −153 kJ mol^{-1}) contributions greatly outweigh Pauli repulsion (441 and 371 kJ mol^{-1}) in **4** and **5**, respectively. The calculated orbital component consists primarily of σ-type donation from Al/Ga to Cu (ca. 50%, Figure 4) along with both σ and π-type back-donation from Cu to Al/Ga (ca. 30%).

The torsion angles between the N(4)−Cu(1)−N(3) and N(2)−Al/Ga(1)−N(1) planes in **4** and **5** (54.34(7) and 54.51(1)°, respectively) suggest the presence of limited π-overlap. This implies that both computational and experimental findings are in accordance with the suggested bonding of an s^2-based lone pair on the group 13 metal, with a minor component from back-donation from the Cu center. LDF interactions are present between the BDI^{Mes} and BDI^{Dip} ligands on the copper and aluminum/gallium fragments, respectively. Selected intramolecular H···H distances between the calculated positions of hydrogen atoms in **4** and **5** with a length shorter than the sum of van der Waals radii (2.4 Å) include some as short as 2.349 and 2.378 Å. It is possible that more short contacts are present in both complexes but due to disorder of the isopropyl groups on one side of the BDI^{Dip} ligand, which is present in both **4** and **5**, these proved difficult to determine. Despite this, computational analyses clearly indicated significant dispersion energies in both complexes. Interestingly, calculations on model systems using Ph groups in place of the Mes and Dip substituents gave rather large interaction enthalpies (189 and 170 kJ mol^{-1} for M = Al and Ga, respectively) even though the contribution from dispersion was found to be greatly decreased (45 and 44 kJ mol^{-1}, respectively). This can be explained with less steric repulsion that allows for more efficient covalent bonding and, therefore, an even shorter calculated Cu−M bond (2.271 and Å in the model systems vs 2.346 and 2.340 Å in **4** and **5**, respectively).

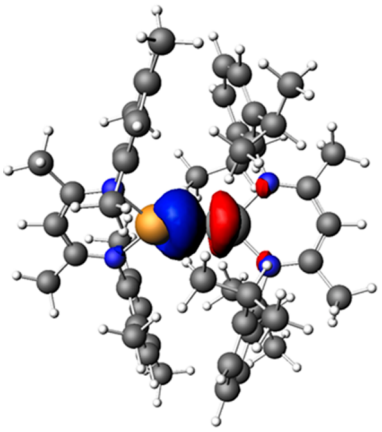

Figure 4. Dominant σ-type ETS-NOCV deformation density contribution to metal−metal bonding in {(BDI^{Mes})CuAl(BDI^{Dip})} (**4**) (isovalue = 0.001 au). Red contour corresponds to depletion of electron density, whereas blue contour indicates accumulation of electron density.

In conclusion, {(BDI^{Mes})CuAl(BDI^{Dip})}, **4**, represents the first example of an unbridged and unsupported Cu−Al bond in a molecular complex. Additionally, its heavier Cu−Ga analogue {(BDI^{Mes})CuGa(BDI^{Dip})}, **5**, has been isolated. Computational analyses at the DFT level showed that **4** and **5** are significantly stabilized by LDFs along with a covalent component including σ-type dative bonding from Al/Ga to Cu and a minor back-donation component from Cu to Al/Ga. Complexes **4** and **5** are currently under investigation for the activation of small molecules including CO and CO$_2$ and the synthesis of species with Cu−(Al/Ga)−O units, which could potentially be used as single-source precursors to deposit copper aluminum and copper gallium oxide thin films.

■ ASSOCIATED CONTENT

Supporting Information

The Supporting Information is available free of charge at https://pubs.acs.org/doi/10.1021/jacs.0c10099.

Experimental and spectroscopic details for complexes **4** and **5**, including NMR spectra and crystallographic parameters, and computational details (PDF)

Crystal data for **4** (CIF)

Crystal data for **5** (CIF)

https://dx.doi.org/10.1021/jacs.0c10099
J. Am. Chem. Soc. XXXX, XXX, XXX−XXX

Accession Codes

Supplementary crystallographic data for complexes **4** and **5** can be accessed from the CCDC using 2022316 and 2022317 respectively. These data can be obtained free of charge via www.ccdc.cam.ac.uk/data_request/cif, or by emailing data_request@ccdc.cam.ac.uk, or by contacting The Cambridge Crystallographic Data Centre, 12 Union Road, Cambridge CB2 1EZ, UK; fax: +44 1223 336033

AUTHOR INFORMATION

Corresponding Author

Philip P. Power − *Department of Chemistry, University of California, Davis, Davis, California 95616, United States;* orcid.org/0000-0002-6262-3209; Email: pppower@ucdavis.edu

Authors

Kristian L. Mears − *Materials Chemistry Centre, Department of Chemistry, University College London, London WC1H 0AJ, United Kingdom;* orcid.org/0000-0002-8515-4177

Cary R. Stennett − *Department of Chemistry, University of California, Davis, Davis, California 95616, United States;* orcid.org/0000-0002-2727-5747

Elina K. Taskinen − *Department of Chemistry, NanoScience Centre, University of Jyväskylä, FI-40014 Jyväskylä, Finland;* orcid.org/0000-0003-3066-7511

Caroline E. Knapp − *Materials Chemistry Centre, Department of Chemistry, University College London, London WC1H 0AJ, United Kingdom;* orcid.org/0000-0003-4219-9313

Claire J. Carmalt − *Materials Chemistry Centre, Department of Chemistry, University College London, London WC1H 0AJ, United Kingdom;* orcid.org/0000-0003-1788-6971

Heikki M. Tuononen − *Department of Chemistry, NanoScience Centre, University of Jyväskylä, FI-40014 Jyväskylä, Finland;* orcid.org/0000-0002-4820-979X

Complete contact information is available at: https://pubs.acs.org/10.1021/jacs.0c10099

Notes

The authors declare no competing financial interest.

ACKNOWLEDGMENTS

We acknowledge the US National Science Foundation (CHE-1565501), the UK Research and Innovation Organization (EP/N509577/1, 1927626) and thank the Royal Society of Chemistry (M19-3658) for their support of this work. This project received funding from the European Research Council (ERC) under the European Union's Horizon 2020 research and innovation programme (grant agreement #772510 to H.M.T.).

REFERENCES

(1) Power, P. P. An Update on Multiple Bonding between Heavier Main Group Elements: The Importance of Pauli Repulsion, Charge-Shift Character, and London Dispersion Force Effects. *Organometallics* **2020**, DOI: 10.1021/acs.organomet.0c00200.

(2) Joy, J.; Danovich, D.; Kaupp, M.; Shaik, S. Covalent vs Charge-Shift Nature of the Metal-Metal Bond in Transition Metal Complexes: A Unified Understanding. *J. Am. Chem. Soc.* **2020**, *142*, 12277−12287.

(3) Powers, I. G.; Uyeda, C. Metal-metal bonds in catalysis. *ACS Catal.* **2017**, *7*, 936−958.

(4) Chipman, J. A.; Berry, J. F. Paramagnetic Metal-Metal Bonded Heterobimetallic Complexes. *Chem. Rev.* **2020**, *120*, 2409−2447.

(5) Power, P. P. Main-group elements as transition metals. *Nature* **2010**, *463*, 171−177.

(6) Berry, J. F.; Lu, C. C. Metal−Metal Bonds: From Fundamentals to Applications. *Inorg. Chem.* **2017**, *56*, 7577−7581.

(7) Moore, J.; Lu, C. C. Catalytic Hydrogenolysis of Aryl C-F Bonds Using a Bimetallic Rhodium-Indium Complex. *J. Am. Chem. Soc.* **2020**, *142*, 11641−11646.

(8) Hicks, J.; Mansikkamäki, A.; Vasko, P.; Goicoechea, J. M.; Aldridge, S. A Nucleophilic Gold Complex. *Nat. Chem.* **2019**, *11*, 237−241.

(9) Wang, Q.; Zhang, S.; Cui, P.; Weberg, A. B.; Thierer, L. M.; Manor, B. C.; Gau, M. R.; Carroll, P. J.; Tomson, N. C. Interdependent Metal-Metal Bonding and Ligand Redox-Activity in a Series of Dinuclear Macrocyclic Complexes of Iron, Cobalt, and Nickel. *Inorg. Chem.* **2020**, *59*, 4200−4214.

(10) Marchand, P.; Sathasivam, S.; Williamson, B. A. D.; Pugh, D.; Bawaked, S. M.; Basahel, S. N.; Obaid, A. Y.; Scanlon, D. O.; Parkin, I. P.; Carmalt, C. J. A Single-Source Precursor Approach to Solution Processed Indium Arsenide Thin Films. *J. Mater. Chem. C* **2016**, *4*, 6761−6768.

(11) Nguyen, T.; Sutton, A. D.; Brynda, M.; Fettinger, J. C.; Long, G. J.; Power, P. P. Synthesis of a Stable Compound with Fivefold Bonding between Two Chromium(I) Centers. *Science* **2005**, *310*, 844−847.

(12) Tsai, Y. C.; Chen, H. Z.; Chang, C. C.; Yu, J. S. K.; Lee, G. H.; Wang, Y.; Kuo, T. S. Journey from Mo-Mo Quadruple Bonds to Quintuple Bonds. *J. Am. Chem. Soc.* **2009**, *131*, 12534−12535.

(13) Das, D.; Mohapatra, S. S.; Roy, S. Recent Advances in Heterobimetallic Catalysis across a "Transition Metal-Tin" Motif. *Chem. Soc. Rev.* **2015**, *44*, 3666−3690.

(14) Gramigna, K. M.; Dickie, D. A.; Foxman, B. M.; Thomas, C. M. Cooperative H_2 Activation across a Metal-Metal Multiple Bond and Hydrogenation Reactions Catalyzed by a Zr/Co Heterobimetallic Complex. *ACS Catal.* **2019**, *9*, 3153−3164.

(15) Cammarota, R. C.; Clouston, L. J.; Lu, C. C. Leveraging Molecular Metal−Support Interactions for H_2 and N_2 Activation. *Coord. Chem. Rev.* **2017**, *334*, 100−111.

(16) Barden, B. A.; Culcu, G.; Krogman, J. P.; Bezpalko, M. W.; Hatzis, G. P.; Dickie, D. A.; Foxman, B. M.; Thomas, C. M. Assessing the Metal-Metal Interactions in a Series of Heterobimetallic Nb/M Complexes (M = Fe, Co, Ni, Cu) and Their Effect on Multielectron Redox Properties. *Inorg. Chem.* **2019**, *58*, 821−833.

(17) Daniels, C. L.; Knobeloch, M.; Yox, P.; Adamson, M. A. S.; Chen, Y.; Dorn, R. W.; Wu, H.; Zhou, G.; Fan, H.; Rossini, A. J.; Vela, J. Intermetallic Nanocatalysts from Heterobimetallic Group 10−14 Pyridine-2-Thiolate Precursors. *Organometallics* **2020**, *39*, 1092−1104.

(18) Hicken, A.; White, A. J. P.; Crimmin, M. R. Selective Reduction of CO_2 to a Formate Equivalent with Heterobimetallic Gold—Copper Hydride Complexes. *Angew. Chem., Int. Ed.* **2017**, *56*, 15127−15130.

(19) Butler, M. J.; White, A. J. P.; Crimmin, M. R. Heterobimetallic Rebound: A Mechanism for Diene-to-Alkyne Isomerization with M—Zr Hydride Complexes (M = Al, Zn, and Mg). *Organometallics* **2018**, *37*, 949−956.

(20) Hicks, J.; Hoyer, C. E.; Moubaraki, B.; Manni, G. L.; Carter, E.; Murphy, D. M.; Murray, K. S.; Gagliardi, L.; Jones, C. A Two-Coordinate Manganese(0) Complex with an Unsupported Mn-Mg Bond: Allowing Access to Low Coordinate Homo- and Heterobimetallic Compounds. *J. Am. Chem. Soc.* **2014**, *136*, 5283−5286.

(21) Garçon, M.; Bakewell, C.; Sackman, G. A.; White, A. J. P.; Cooper, R. I.; Edwards, A. J.; Crimmin, M. R. A Hexagonal Planar Transition-Metal Complex. *Nature* **2019**, *574*, 390−393.

(22) Lei, H.; Guo, J. D.; Fettinger, J. C.; Nagase, S.; Power, P. P. Two-Coordinate First Row Transition Metal Complexes with Short Unsupported Metal-Metal Bonds. *J. Am. Chem. Soc.* **2010**, *132*, 17399−17401.

(23) Burns, C. P.; Yang, X.; Wofford, J. D.; Bhuvanesh, N. S.; Hall, M. B.; Nippe, M. Structure and Magnetization Dynamics of Dy−Fe

and Dy−Ru Bonded Complexes. *Angew. Chem.* **2018**, *130*, 8276−8280.
(24) Doddi, A.; Peters, M.; Tamm, M. N-Heterocyclic Carbene Adducts of Main Group Elements and Their Use as Ligands in Transition Metal Chemistry. *Chem. Rev.* **2019**, *119*, 6994−7112.
(25) Zhou, Y. P.; Driess, M. Isolable Silylene Ligands Can Boost Efficiencies and Selectivities in Metal-Mediated Catalysis. *Angew. Chem., Int. Ed.* **2019**, *58*, 3715−3728.
(26) Roesky, P. W. Compounds with Low-Valent Group 13 Metals as Ligands for Electron Poor Main Group and Transition Metals. *Dalt. Trans.* **2009**, 1887−1893.
(27) Dohmeier, C.; Loos, D.; Schnöckel, H. Aluminum(I) and Gallium(I) Compounds: Syntheses, Structures, and Reactions. *Angew. Chem., Int. Ed. Engl.* **1996**, *35*, 129−149.
(28) Hobson, K.; Carmalt, C. J.; Bakewell, C. Recent Advances in Low Oxidation State Aluminium Chemistry. *Chem. Sci.* **2020**, *11*, 6942−6956.
(29) Asay, M.; Jones, C.; Driess, M. N-Heterocyclic Carbene Analogues with Low-Valent Group 13 and Group 14 Elements: Syntheses, Structures, and Reactivities of a New Generation of Multitalented Ligands. *Chem. Rev.* **2011**, *111*, 354−396.
(30) Puls, A.; Jerabek, P.; Kurashige, W.; Förster, M.; Molon, M.; Bollermann, T.; Winter, M.; Gemel, C.; Negishi, Y.; Frenking, G.; Fischer, R. A. A Novel Concept for the Synthesis of Multiply Doped Gold Clusters $[(M@Au_nM'_m)L_k]^{q+}$. *Angew. Chem., Int. Ed.* **2014**, *53*, 4327−4331.
(31) Ganesamoorthy, C.; Weßing, J.; Kroll, C.; Seidel, R. W.; Gemel, C.; Fischer, R. A. The Intermetalloid Cluster $[(Cp^*AlCu)_6H_4]$, Embedding a Cu_6 Core inside an Octahedral Al_6 Shell: Molecular Models of Hume-Rothery Nanophases. *Angew. Chem., Int. Ed.* **2014**, *53*, 7943−7947.
(32) Dange, D.; Choong, S. L.; Schenk, C.; Stasch, A.; Jones, C. Synthesis and Characterisation of Anionic and Neutral Gallium(I) N-Heterocyclic Carbene Analogues. *Dalt. Trans.* **2012**, *41*, 9304−9315.
(33) Hardman, N. J.; Eichler, B. E.; Power, P. P. Synthesis and Characterization of the Monomer $Ga\{(NDipCMe)_2CH\}$ (Dip = $C_6H_3Pr(i)_2$-2,6): A Low Valent Gallium(I) Carbene Analogue. *Chem. Commun.* **2000**, 1991−1992.
(34) Green, S. P.; Jones, C.; Mills, D. P.; Stasch, A. Group 9 and 11 Metal(I) Gallyl Complexes Stabilized by N-Heterocyclic Carbene Coordination: First Structural Characterization of Ga-M (M = Cu or Ag) Bonds. *Organometallics* **2007**, *26*, 3424−3430.
(35) Jones, C.; Stasch, A.; Moxey, G. J.; Junk, P. C.; Deacon, G. B. Complexes of Four-Membered Group 13 Metal(I) N-Heterocyclic Carbene Analogues with Metal Carbonyl Fragments. *Eur. J. Inorg. Chem.* **2009**, *24*, 3593−3599.
(36) Moxey, G. J.; Jones, C.; Stasch, A.; Junk, P. C.; Deacon, G. B.; Woodul, W. D.; Drago, P. R. Complexes of Four-Membered Group 13 Metal(I) N-Heterocyclic Carbene Analogues with Platinum(II) Fragments. *Dalton Trans.* **2009**, *14*, 2630−2636.
(37) Jones, C.; Mills, D. P.; Rose, R. P.; Stasch, A.; Woodul, W. D. Synthesis and Further Reactivity Studies of Some Transition Metal Gallyl Complexes. *J. Organomet. Chem.* **2010**, *695*, 2410−2417.
(38) Xie, W.; Heo, J.; Kim, D.; Chang, S. Copper-Catalyzed Direct C−H Alkylation of Polyfluoroarenes by Using Hydrocarbons as an Alkylating Source. *J. Am. Chem. Soc.* **2020**, *142*, 7487−7496.
(39) Cui, C.; Roesky, H. W.; Schmidt, H.; Noltemeyer, M.; Hao, H.; Cimpoesu, F. Synthesis and Structure of a Monomeric Aluminum(I) Compound $[\{HC(CMeNAr)_2\}Al]$ (Ar = 2,6−$IPr_2C_6H_3$): A Stable Aluminum Analogue of a Carbene. *Angew. Chem.* **2000**, *112*, 4444−4446.
(40) Hardman, N. J.; Phillips, A. D.; Power, P. P. Bonding and Reactivity of a *β*-Diketiminate, Gallium(I), Carbene Analogue. Group 13 Chemistry: From Fundamentals to Applications. *ACS Symp. Ser. Am. Chem. Soc.* **2002**, *822*, 2−15.

https://dx.doi.org/10.1021/jacs.0c10099
J. Am. Chem. Soc. XXXX, XXX, XXX−XXX